

## Infrared reflectance spectra and dispersion studies of iron-intercalated zirconium diselenide

M. T. Ratajack\* and C. R. Kannewurf

*Department of Electrical Engineering and Materials Research Center, Northwestern University, Evanston, Illinois 60201*

J. F. Revelli† and J. B. Wagner‡

*Department of Material Science and Materials Research Center, Northwestern University, Evanston, Illinois 60201*

(Received 18 October 1977)

Infrared reflectance spectra for numerous compositions of the intercalation system  $\text{Fe}_x\text{ZrSe}_2$  have been measured and analyzed in terms of a Lorentzian oscillator model. The analysis has indicated that no new vibrational modes resulted as a consequence of iron intercalation and that the single TO-phonon frequency observed for the host spectrum was invariant with iron concentration. The intercalated samples showed a linear increase in electronic polarizability with iron concentration as well as increases in oscillator strength and damping. These results are discussed in terms of a model in which the iron acts only to modify the oscillator parameters of  $\text{ZrSe}_2$ .

### I. INTRODUCTION

Recently there has been a considerable amount of interest in layered-transition-metal dichalcogenide (LTMD) systems where studies have indicated that the physical properties of the host material may be dramatically altered by the intercalation of foreign atoms or molecules.<sup>1-3</sup> These studies have led to a variety of new quasibinary systems of the form  $M_xTX_2$ , where  $T$  is a transition metal,  $X$  is S, Se, or Te, and the intercalate  $M$  can be either an alkali metal, a transition metal, or a post-transition metal. Numerous investigations of the electrical conduction and crystallographic properties of these systems have indicated that a wide range of characteristics can be obtained by varying the guest species ( $M$ ), the concentration of the guest species ( $x$ ), as well as the layered host lattice itself ( $TX_2$ ).

Presently, studies of the optical dielectric properties of LTMD systems have been limited primarily to investigations of unintercalated compounds of the form  $TX_2$ .<sup>4,5</sup> The infrared reflectance spectra of many group-IV and group-VI transition-metal dichalcogenides have been reported by Lucovsky *et al.*<sup>5</sup> The spectra were found to be of three basic types: very strong reststrahl for  $\text{ZrS}_2$ ,  $\text{HfS}_2$ , and  $\text{HfSe}_2$ ; weaker reststrahl for  $\text{MoS}_2$ ,  $\text{MoSe}_2$ ,  $\text{WS}_2$ , and  $\text{WSe}_2$ ; and plasmon-type reflection for  $\text{TiS}_2$ ,  $\text{ZrTe}_2$ , and  $\text{HfTe}_2$ . A Lorentzian oscillator dispersion analysis technique was used by these authors to obtain information regarding the infrared-active optical vibrational modes and an effective charge parameter for these materials. The results thus obtained were then used in a discussion of the bonding mechanism in LTMD crystals. Although many LTMD intercalation systems have been studied electrically and crystallographically, little or no information is

currently available about the effect of intercalation upon the infrared-active modes in these systems.

In this paper a study of the far-infrared reflectance spectra for the  $\text{Fe}_x\text{ZrSe}_2$  system is presented as a function of the intercalate iron concentration. This system has been found to exist in two distinct phases: a semiconducting phase for  $0 \leq x < \frac{1}{3}$  and a metallic phase for  $x \approx \frac{1}{2}$ .<sup>6</sup> For this study both single-crystal and pressed-pellet samples in the range  $0 \leq x \leq 0.26$  (semiconducting phase) were used. Some details of the sample preparation and crystallographic characterization are presented in Sec. II along with a discussion of the infrared-active modes pertinent to this system. The infrared reflectance spectra and dispersion analysis are presented in Sec. III and a discussion of the results is given in Sec. IV.

### II. SAMPLE PREPARATION AND CRYSTALLOGRAPHY

Samples of the  $\text{Fe}_x\text{ZrSe}_2$  system were prepared by the method of chemical vapor transport. Appropriate quantities of the elements Fe (99.5% purity), Zr (99.9% purity), and Se (99.9999% purity) were weighed out and placed in quartz ampoules which were then evacuated to approximately  $10^{-3}$  torr. Following the addition of approximately 120-torr partial pressure of hydrogen chloride gas as a transport agent, the ampoules were sealed and heated uniformly to 450°C for several days. After transporting for two weeks in a temperature gradient of 935–840°C the samples were slowly cooled and removed from the furnaces. The single-phase semiconducting material was obtained when the initial Fe to Zr ratio was less than  $\frac{1}{3}$  and a compositional analysis was performed by means of x-ray fluorescence. This analysis indicated that in most samples the actual concentration of iron was somewhat below the nominal com-

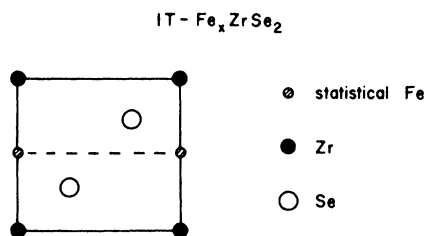


FIG. 1. View in the (110) plane of the crystal structure of semiconducting Fe<sub>x</sub>ZrSe<sub>2</sub>.

position indicated by the initial Fe to Zr ratio. This discrepancy is attributed to partial reaction of the iron with the quartz reaction vessels.

The results of single-crystal x-ray diffraction analysis, reported by Gleizes *et al.*,<sup>7</sup> indicate that throughout the range  $0 \leq x < 0.26$  the symmetry space group  $D_{3d}^3-P\bar{3}m1$  is retained with the intercalated iron atoms distributed randomly in the octahedral holes between Se-Zr-Se layers. The structure is a variation of the CdI<sub>2</sub>-NiAs intermediate type with both  $c$  and  $a$  parameters remaining constant throughout ( $6.118 \leq c \leq 6.133$  Å and  $3.763 \leq a \leq 3.773$  Å). This structure is depicted in Fig. 1.

A group-theoretical analysis of the  $\Gamma$  point lattice modes for the basic 1T-ZrSe<sub>2</sub> structure (symmetry  $D_{3d}$ ) has been carried out.<sup>8</sup> That analysis shows that the three atoms per unit cell result in a decomposition into irreducible representations at the Brillouin-zone center  $\Gamma$  as follows:

$$\Gamma = A_{1g} + E_g + 2A_{2u} + 2E_u. \quad (1)$$

Of these modes, only the  $A_{2u}$  (corresponding to  $\vec{E} \parallel \vec{c}$  polarization) and the  $E_u$  (corresponding to  $\vec{E} \perp \vec{c}$  polarization) modes will be infrared active. These two optical-mode motions are represented in Fig. 2. Up to this point, the presence of the interstitial iron atoms have not been taken into account. In view of the results of the single-crystal x-ray analysis; namely, that the crystal symmetry  $D_{3d}$  is preserved throughout the composition range of the semiconducting phase of Fe<sub>x</sub>ZrSe<sub>2</sub>, the same irreducible representations for the vibrational modes at the  $\Gamma$  point that were obtained for

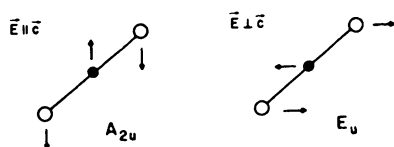


FIG. 2. Infrared-active mode motions for the structure of 1T-ZrSe<sub>2</sub>.

the host material are expected for the intercalated material. As will be discussed in the subsequent sections, this has in fact been observed experimentally to be the case.

### III. REFLECTANCE SPECTRA AND DISPERSION ANALYSIS

All measurements of the reflectance spectra for various compositions of the semiconducting phase of the Fe<sub>x</sub>ZrSe<sub>2</sub> system were made using a Perkin-Elmer model 180 infrared spectrophotometer. The instrument was operated in the double-beam mode and calibration was accomplished by use of a front surface gold mirror. Measurements in the frequency range 525–4000 cm<sup>-1</sup> were made using a globar source and a thermopile detector while an Hg source and a pyroelectric detector were used for frequencies less than 525 cm<sup>-1</sup>. All measurements were made at room temperature using unpolarized radiation at near-normal incidence ( $\sim 20^\circ$ ).

Both single-crystal and pressed-pellet samples were used in the measurement of the reflectance spectra. Since the crystalline samples were typically thin platelets with the crystallographic  $c$  axis oriented perpendicular to the platelet surface, only spectra with the polarization  $\vec{E} \perp \vec{c}$  could be obtained (i.e., the  $E_u$  mode). For pellets pressed from crystalline powders, a significant alignment of the  $c$  axes was expected due to the platelike nature of the individual grains. Other authors have reported that pellets of other LTMD systems prepared in a similar manner have had 90% of the crystallites in the pellet aligned with  $10^\circ$  of normal to the pellet surface.<sup>5</sup> For this reason, the excitation of modes other than the  $E_u$  mode in pellet samples was expected to be nearly negligible. This is demonstrated by a comparison of the spectra obtained for a single crystal and pressed pellet of the host material ZrSe<sub>2</sub>, as shown in Fig. 3. The only significant difference is the appearance of a

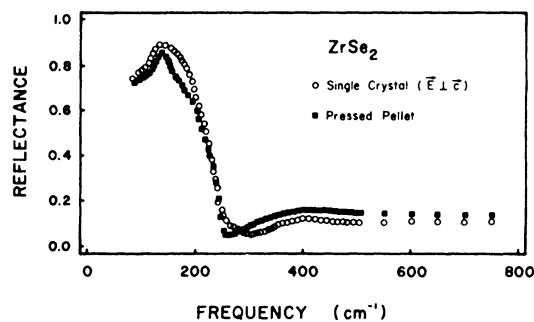


FIG. 3. Comparison of the room-temperature reflectance spectra for a single crystal and a pressed pellet of ZrSe<sub>2</sub>.

sharp peak in the spectrum of the pellet sample in the vicinity of maximum reflectance. This was characteristic of all pellet samples examined and may possibly be attributed to a small excitation of the  $A_{2u}$  mode in these samples. However, other similarities in reflectance spectra and the fitted oscillator parameters suggest that the  $\vec{E} \perp \vec{c}$  polarization predominates in the pellet sample.

Both a Kramers-Kronig and a Lorentzian oscillator dispersion analysis were performed on all samples examined. The Kramers-Kronig analysis was used to insure the Lorentzian character of the measured reflectance spectra and to detect the presence of any possible vibrational modes other than the  $E_u$  mode associated with the host  $ZrSe_2$  in the iron intercalated samples. This analysis employed the Kramers-Kronig relation between the magnitude and the phase of the complex reflection coefficient

$$r = (n^* - 1)/(n^* + 1) = |r| e^{-i\phi}, \quad (2)$$

where  $n^* = n - ik$  is the complex index of refraction. A computer program was used to solve the familiar integral

$$\phi(\omega_0) = \frac{1}{2\pi} \int_0^\infty \ln \left| \frac{\omega - \omega_0}{\omega + \omega_0} \right| \frac{d}{d\omega} \ln R \, d\omega, \quad (3)$$

where  $R = |r|^2$  represents the measured reflectance and the frequency dependencies of the real and imaginary parts of the complex dielectric permittivity,  $\epsilon^* = \epsilon_1 - i\epsilon_2$ , as well as the energy-loss function,  $\text{Im}(1/\epsilon^*)$ , were determined by noting that  $n^* = \sqrt{\epsilon^*}$ . Since the positions of the peaks in  $\epsilon_2$  and  $\text{Im}(1/\epsilon^*)$  locate the TO- and LO-phonon frequencies, respectively, the presence of additional vibrational modes due to the intercalated iron could be easily identified. In fact no such modes were found over the range 50–4000  $\text{cm}^{-1}$ . All of the intercalated samples showed only a single peak in  $\epsilon_2$  which was coincident in frequency with the peak in  $\epsilon_2$  observed for the unintercalated  $ZrSe_2$ . Consequently,

it was concluded that the data could be analyzed in terms of a model in which the intercalate iron acts only to modify the oscillator parameters of the host  $ZrSe_2$ .

The oscillator analysis was accomplished by fitting the experimentally measured reflectance spectrum of each sample to a theoretically synthesized spectrum obtained by modeling the complex dielectric permittivity as a superposition of damped Lorentzian oscillators

$$\epsilon^* = \epsilon_\infty + \sum_j \frac{S_j \omega_{0j}^2}{\omega_{0j}^2 - \omega^2 - i\gamma_j \omega_{0j} \omega}, \quad (4)$$

where  $\epsilon_\infty$  is the high-frequency dielectric constant and  $\omega_{0j}$ ,  $S_j$ , and  $\gamma_j$  are the frequency, strength, and damping of the  $j$ th oscillator. The theoretical spectrum is then synthesized by

$$R = |(\sqrt{\epsilon^*} - 1)/(\sqrt{\epsilon^*} + 1)|^2, \quad (5)$$

and fit to the experimental data by allowing the oscillator parameters to vary. The fitting procedure was done by means of a computer program which used a modified Gauss-Newton nonlinear least-squares estimation technique incorporated with an iterative search to obtain values of the oscillator parameters which minimized the rms deviation between the synthesized and experimental spectra.<sup>9</sup> The analysis was carried out using only a single Lorentzian oscillator (as suggested by the Kramers-Kronig results) and a summary of the fitted oscillator parameters for the  $Fe_xZrSe_2$  system is given in Table I. In all cases the rms deviation between the experiment and fit was less than 0.04.

Representative reflectance spectra and Lorentzian oscillator fits for the  $Fe_xZrSe_2$  system are shown in Fig. 4. In each case the experimental spectrum is represented by data points while the solid line is used to represent the spectrum obtained from the oscillator model. The host (unintercalated) spectrum shows a strong reststrahl

TABLE I. Oscillator parameters as a function of iron concentration and effective charge normalized to that of  $ZrSe_2$  ( $\sim 4e$ ).

| Composition<br>$x$ | Oscillator parameters<br>( $\text{cm}^{-1}$ ) |               |       |            | Normalized<br>effective charge<br>$e_{\text{eff}}^*/e_{\text{Zr}}^*$ ( $x=0$ ) |
|--------------------|---|---------------|-------|------------|--|
|                    | $\epsilon_\infty$                             | $\omega_{01}$ | $S_1$ | $\gamma_1$ |  |
| 0.000              | 6.78  | 102           | 33.0  | 0.294      | 1.00   |
| 0.038              | 9.71  | 106           | 36.8  | 0.347      | 1.10   |
| 0.070              | 9.80  | 102           | 43.0  | 0.320      | 1.14   |
| 0.116              | 11.46   | 102           | 46.3  | 0.635      | 1.18   |
| 0.134              | 11.94   | 102           | 48.5  | 0.739      | 1.12   |
| 0.142              | 13.43   | 104           | 55.9  | 0.733      | 1.33   |
| 0.193              | 15.18   | 102           | 60.4  | 0.744      | 1.35   |
| 0.263              | 15.63   | 102           | 70.6  | 0.765      | 1.46   |

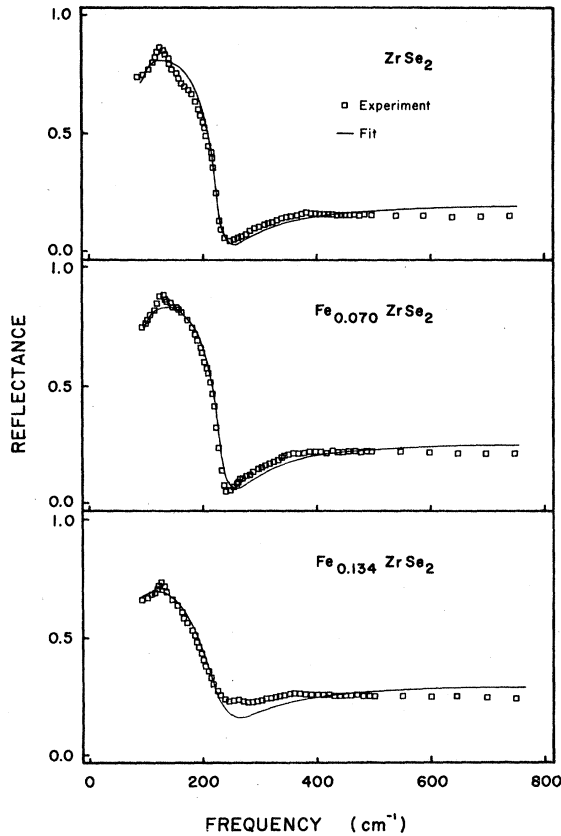


FIG. 4. Typical room-temperature reflectance spectra (data points) and oscillator fits (solid lines) for pressed pellets of the  $\text{Fe}_x\text{ZrSe}_2$  system.

with characteristic features very similar to those reported for  $\text{HfSe}_2$ .<sup>5</sup> The remaining two intercalated spectra ( $x=0.070$  and  $x=0.134$ ) show qualitative features quite similar to the host but indicate, however, a significant change in the high-frequency dielectric constant, the oscillator strength, and damping over those obtained for  $\text{ZrSe}_2$ . These

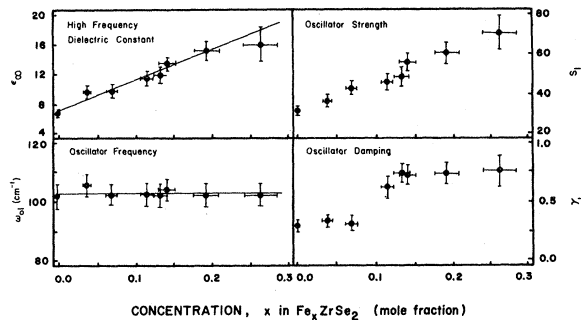


FIG. 5. Variation of the single Lorentzian oscillator parameters with iron concentration.

changes are depicted graphically in Fig. 5. The deviation between the experiment and fit about the reflectance minimum for  $x=0.134$  was typical of all samples examined with iron concentrations greater than 10%.

#### IV. DISCUSSION

In this section the variation of the oscillator parameters with the intercalate iron concentration will be discussed. The first parameter to be discussed is the oscillator frequency  $\omega_{01}$ . As has been described in the previous sections, the oscillator frequency is observed to have a compositionally independent value of  $102 \pm 4 \text{ cm}^{-1}$ . This observation is consistent with a model in which the oscillator frequency is determined by the reduced mass of the zirconium-selenium oscillator ( $m_r$ ) and an effective force constant ( $k_{\text{eff}}$ ) as

$$\omega_0^2 = k_{\text{eff}}/m_r, \quad (6)$$

where

$$m_r = m_{\text{Zr}}m_{\text{Se}}/(m_{\text{Zr}} + 2m_{\text{Se}}), \quad (7)$$

since neither the reduced mass nor force constant is expected to vary with iron concentration. In general this "spring constant" model for the oscillator frequency is inadequate because it ignores the interactions between oscillators that reside on the lattice sites. These interactions generally result in a reduction of the transverse optical frequency from that given by Eq. (6) by an amount that will be a function of the effective charge parameter  $e_T^*$  as follows<sup>5,10</sup>:

$$\omega_0^2 - \omega_{\text{TO}}^2 = f(e_T^*). \quad (8)$$

Since  $\omega_0$  is not expected to vary with iron concentration and  $\omega_{\text{TO}} = \omega_{01}$  has been observed as compositionally independent, the function  $f(e_T^*)$  should be constant for the semiconducting phase of the  $\text{Fe}_x\text{ZrSe}_2$  system.

The high-frequency dielectric constant  $\epsilon_\infty$  is observed to increase with iron concentration. This term is the result of residual polarizability at high frequencies due to electronic oscillations which typically have a resonant frequency much higher than the ionic oscillation frequency. If a simplistic model in which the electrons are confined to a cloud of radius  $r_e$  surrounding the atom is assumed,<sup>11</sup> then this parameter may be expressed as<sup>9</sup>

$$\epsilon_\infty = 1 + 4\pi r_e^3 N_e, \quad (9)$$

where  $N_e$  represents the density of electronic oscillators. For the  $\text{Fe}_x\text{ZrSe}_2$  system,  $N_e$  may be expressed as a summation of two contributions; the first being a compositionally independent term accounting for the polarizability of the host  $\text{ZrSe}_2$  and

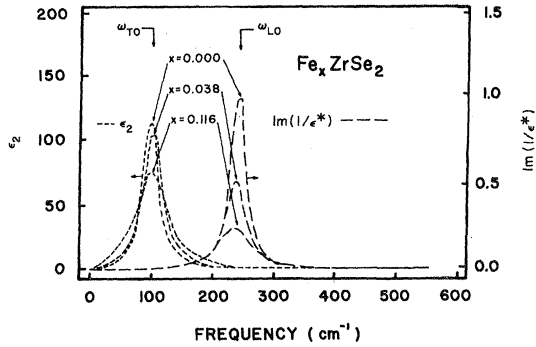


FIG. 6. Frequency dependence of  $\epsilon_2$  and  $\text{Im}(\epsilon^{-1})$  obtained from the oscillator model for several compositions of  $\text{Fe}_x\text{ZrSe}_2$ .

the second being a function of the iron concentration, accounting for the polarizability of the intercalate iron. Since the crystallographic parameters for the semiconducting phase are invariant with iron concentration, an increase in  $x$  will result in a linear increase in the density of electronic oscillators. Consequently, a linear variation of  $\epsilon_\infty$  with iron concentration is expected, as shown in Fig. 5. It is unlikely that this increase is due to appreciable free-carrier effects since that even at the highest iron concentration no plasmon modes were observed in this system; which is consistent with studies of the electrical conduction properties of semiconducting  $\text{Fe}_x\text{ZrSe}_2$ .<sup>6</sup>

An examination of the Lyddane-Sachs-Teller equation<sup>12</sup> relating TO- and LO-phonon frequencies to the static and high-frequency dielectric constants yields information regarding the variation of the oscillator strength

$$\omega_{\text{LO}}^2/\omega_{\text{TO}}^2 = \epsilon(0)/\epsilon_\infty. \quad (10)$$

Physically, the oscillator strength represents the change in dielectric constant upon passing through the reststrahlen band so that the static dielectric constant may be expressed as  $\epsilon(0) = \epsilon_\infty + S_1$ . The two phonon frequencies have been found to be virtually independent of iron concentration (see Fig. 6) being determined by the modes of the host lattice. Consequently, in this case, the increase in the oscillator strength with iron concentration may be attributed to the aforementioned increase in electronic polarizability.

Figure 6 demonstrates the effect of iron intercalation upon the oscillator damping. Qualitatively, the effect may be described as a broadening and suppression of the normal  $E_u$  mode of  $\text{ZrSe}_2$  due to the lowered local symmetry and additional impurity damping. The trend is toward an increase in damping with an increase in iron concentration although the change is not as regular as has been observed

in the other oscillator parameters. This may possibly be attributable to small variations in the measured maximum reflectance from sample to sample.

The analysis of the reflectance spectra of  $\text{Fe}_x\text{ZrSe}_2$  by means of the Lorentzian oscillator model leads to a discussion of this system in terms of an effective charge parameter. This parameter is defined as

$$e_T^* \equiv \left. \frac{\partial p}{\partial u} \right|_E, \quad (11)$$

where  $p$  is the electric dipole moment induced by a displacement ( $u$ ) of the atoms from their equilibrium positions and  $E$  is the macroscopic electric field. In terms of the oscillator model,  $e_T^*$  becomes

$$e_T^* = (m_r \epsilon_0 S_1 / N_0)^{1/2} \omega_{01}, \quad (12)$$

where  $m_r$  is the mode mass given by Eq. (7),  $\epsilon_0$  is the permittivity of free space,  $N_0$  is the density of oscillators, and  $S_1$  and  $\omega_{01}$  are oscillator parameters. For unintercalated  $\text{ZrSe}_2$  one finds  $e_T^* \approx 4e$  which is consistent with the ionic character of this material.<sup>13</sup>

The results for the intercalated samples show a monotonic increase in the effective charge parameter with iron concentration. This may be taken as evidence for the strong ionicity of the semiconducting phase, as suggested in Ref. 7. Furthermore, this may be viewed as a consequence of the increase in electronic polarizability due to the intercalated iron by an examination of Eq. (8). The invariance of  $f(e_T^*)$ , which represents a reduction in the TO-phonon frequency from that which would be expected from a "spring constant" model, has been previously argued for the semiconducting phase. Since in the case when electronic excitations are considered to be localized, one finds<sup>5,14</sup>

$$f(e_T^*) \propto e_T^{*2} / \epsilon_\infty + 2$$

the increase in  $\epsilon_\infty$  with  $x$  must be accompanied by an increase in  $e_T^*$  to maintain the same TO-phonon frequency at all iron concentrations. This dependence of  $e_T^*$  is shown in Fig. 7.

In summary, the infrared reflectance spectra of the semiconducting phase of  $\text{Fe}_x\text{ZrSe}_2$  has been studied as a function of iron concentration. The results of the subsequent dispersion analyses may be summarized as follows. A single reststrahlen band was observed for the unintercalated host material with  $\omega_{\text{TO}} = 102 \text{ cm}^{-1}$ . A Kramers-Kronig analysis of all iron intercalated samples showed only a single transverse-optical phonon frequency which was very close to that for the host  $\text{ZrSe}_2$ . From this result it was concluded that no additional vibrational modes were present due to the interca-

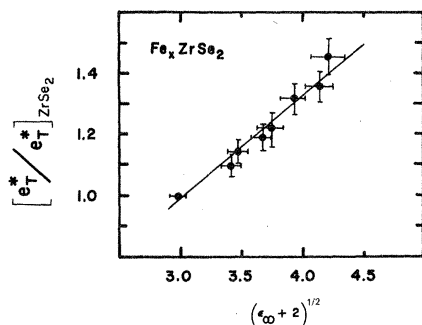


FIG. 7. Representation of the variation in the effective charge parameter normalized to that of  $ZrSe_2$  with the high-frequency polarizability as suggested in the text.

lation of iron. The electronic polarizability of the intercalation complex was observed to increase linearly with iron concentration and this was attributed to electronic oscillations of Fe atoms within the Van der Waals gap. The oscillator strength and damping were also found to increase with iron concentration. As a consequence of the increase both in electronic polarizability and oscillator strength with a compositionally independent oscillator frequency, the macroscopic effective charge parameter showed a monotonic increase

with iron concentration beyond that of  $ZrSe_2$ .

Finally, it should be noted that many of the qualitative effects of intercalation upon the infrared reflectance spectra of  $Fe_xZrSe_2$  reported in this paper have also been observed in preliminary measurements of other LTMD intercalation systems.<sup>15</sup> In particular, studies now in progress of the  $Fe_xTiSe_2$  system have initially indicated an increase in electronic polarizability with iron concentration which is very similar to the variation obtained for  $Fe_xZrSe_2$ . The remainder of the dispersion analysis is somewhat more complicated due to the semimetallic nature of the system.<sup>16</sup> A preliminary Kramers-Kronig analysis of a few selected compositions has suggested that the spectra are best modeled by a dielectric permittivity which includes plasmon modes as well as Lorentzian oscillator modes. This is at least in qualitative agreement with results that have been recently reported for  $TiSe_2$ .<sup>17-20</sup>

#### ACKNOWLEDGMENTS

The authors wish to thank Dr. R. Zallen of Xerox Corporation for suggesting improvements in the analysis techniques. This research was supported by the NSF through the Materials Research Center at Northwestern University.

\*Present address: Dept. of Information Engineering, University of Illinois at Chicago Circle, Chicago, Ill. 60680.

†Present address: Xerox Corporation, Webster Research Center, Webster, N. Y. 14580.

‡Present address: Arizona State University, Center for Solid State Sciences, Tempe, Ariz. 85281.

<sup>1</sup>F. R. Gamble, F. J. DiSalvo, R. A. Klemm, and T. H. Geballe, *Science* **168**, 568 (1970).

<sup>2</sup>J. J. Hauser, M. Robbins, and F. J. DiSalvo, *Phys. Rev. B* **8**, 1038 (1973).

<sup>3</sup>R. M. Fleming and R. V. Coleman, *Phys. Rev. Lett.* **34**, 1502 (1975).

<sup>4</sup>A. S. Barker, Jr., J. A. Ditzenberger, and F. J. DiSalvo, *Phys. Rev. B* **12**, 2049 (1975).

<sup>5</sup>G. Lucovsky, R. M. White, J. A. Benda, and J. F. Revelli, *Phys. Rev. B* **7**, 3859 (1973).

<sup>6</sup>M. T. Ratajack, J. F. Revelli, J. B. Wagner, and C. R. Kannewurf, *Bull. Am. Phys. Soc.* **22**, 422 (1977).

<sup>7</sup>A. Gleizes, J. Revelli, and J. A. Ibers, *J. Solid State Chem.* **17**, 363 (1976).

<sup>8</sup>P. J. Lockwood, in *Light Scattering in Solids*, edited by G. B. Wright (Springer, New York, 1969), p. 75.

<sup>9</sup>M. T. Ratajack, Ph.D. dissertation (Northwestern University, 1977) (unpublished).

<sup>10</sup>G. Lucovsky, R. M. Martin, and E. Burstein, *Phys. Rev. B* **4**, 1367 (1971).

<sup>11</sup>E. C. Jordan and K. G. Balmain, *Electromagnetic Waves and Radiating Systems*, (Prentice-Hall, Englewood Cliffs, N. J., 1968), p. 298.

<sup>12</sup>D. H. Martin, *Adv. Phys.* **14**, 39 (1965).

<sup>13</sup>R. M. White and G. Lucovsky, *Solid State Commun.* **11**, 1369 (1972).

<sup>14</sup>E. Burstein, A. Pinczuk, and R. F. Wallis, in *Proceedings of the Conference of the Physics of Semimetals and Narrow Gap Semiconductors*, edited by D. L. Carter and R. T. Bate (Pergamon, New York, 1971), p. 251.

<sup>15</sup>J. W. Lyding, C. R. Kannewurf, J. F. Revelli, and M. T. Ratajack (unpublished).

<sup>16</sup>M. T. Ratajack, J. W. Lyding, C. R. Kannewurf, and J. F. Revelli, *Extended Abstracts* (Electrochemical Soc., Princeton, N. J., 1977), Vol. 77-2, p. 811.

<sup>17</sup>G. Lucovsky, R. M. White, and Y. S. Liang, *Bull. Am. Phys. Soc.* **21**, 225 (1976).

<sup>18</sup>G. Lucovsky, W. Y. Liang, R. M. White, and K. R. Pisharody, *Solid State Commun.* **19**, 303 (1976).

<sup>19</sup>W. Y. Liang, G. Lucovsky, R. M. White, W. Stutius, and K. R. Pisharody, *Philos. Mag.* **33**, 493 (1976).

<sup>20</sup>G. Lucovsky, R. M. White, W. Y. Liang, and J. C. Mikkelsen, *Philos. Mag.* **34**, 907 (1976).